Developmental Cognitive Neuroscience 66 (2024) 101373

Contents lists available at ScienceDirect

Developmental Cognitive Neuroscience

journal homepage: www.elsevier.com/locate/dcn

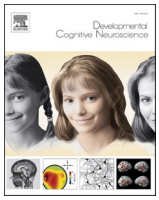

Aperiodic EEG and 7T MRSI evidence for maturation of E/I balance supporting the development of working memory through adolescence

Shane D. McKeon [a,b,1,*], Maria I. Perica [b,c], Ashley C. Parr [b,d], Finnegan J. Calabro [a,b,d], Will Foran [d], Hoby Hetherington [e,f], Chan-Hong Moon [g], Beatriz Luna [b,d,**]

[a] Department of Bioengineering, University of Pittsburgh, PA, USA
[b] The Center for the Neural Basis of Cognition, University of Pittsburgh, PA, USA
[c] Department of Psychology, University of Pittsburgh, PA, USA
[d] Department of Psychiatry, University of Pittsburgh, PA, USA
[e] Resonance Research Incorporated, Billerica, MA, USA
[f] Department of Radiology, University of Missouri, Columbia, MO, USA
[g] Department of Radiology, University of Pittsburgh, PA, USA

ARTICLE INFO

Keywords:
EEG
Adolescent development
Aperiodic activity
GABA
Glutamate
Excitation/Inhibition balance

ABSTRACT

Adolescence has been hypothesized to be a critical period for the development of human association cortex and higher-order cognition. A defining feature of critical period development is a shift in the excitation: inhibition (E/I) balance of neural circuitry, however how changes in E/I may enhance cortical circuit function to support maturational improvements in cognitive capacities is not known. Harnessing ultra-high field 7 T MR spectroscopy and EEG in a large, longitudinal cohort of youth (N = 164, ages 10–32 years old, 347 neuroimaging sessions), we delineate biologically specific associations between age-related changes in excitatory glutamate and inhibitory GABA neurotransmitters and EEG-derived measures of aperiodic neural activity reflective of E/I balance in prefrontal association cortex. Specifically, we find that developmental increases in E/I balance reflected in glutamate:GABA balance are linked to changes in E/I balance assessed by the suppression of prefrontal aperiodic activity, which in turn facilitates robust improvements in working memory. These findings indicate a role for E/I-engendered changes in prefrontal signaling mechanisms in the maturation of cognitive maintenance. More broadly, this multi-modal imaging study provides evidence that human association cortex undergoes physiological changes consistent with critical period plasticity during adolescence.

1. Introduction

Prefrontal cortex (PFC) undergoes significant maturation through adolescence, including gray matter thinning (Paus et al., 2008; Whitford et al., 2007; Giedd, 2004) and changes in task-related activation (Luna et al., 2015, 2001; Bunge et al., 2002; Ciesielski et al., 2006). In parallel, cognitive control is being refined through adolescence following steep improvements from early childhood (Tervo-Clemmens et al., 2022). Both PFC maturation and cognitive development become stabilized in adulthood, indicating the end of a phase of active specialization that may reflect earlier plasticity (Murty et al., 2016). Recently, it has been proposed that adolescence is a developmental critical period for the PFC and its associated functionality (Larsen and Luna, 2018). Supporting this hypothesis are studies in rodent models (Chattopadhyaya et al., 2004; Micheva and Beaulieu, 1997) and postmortem human tissue (Mauney et al., 2013; Fung et al., 2010) that have shown mechanistic changes consistent with critical period plasticity, including increases in inhibitory, GABAergic parvalbumin (PV) interneurons and decreases in excitatory, glutamatergic processes, resulting in changes in excitation/inhibition (E/I) balance (Caballero et al., 2021), a hallmark of critical period plasticity (Hensch, 2005). Motivated by these initial findings, we previously used high field 7 T MRSI to measure cross-sectional age related changes through adolescence into adulthood in the correspondence of glutamate and GABA function finding evidence of increases in

* Corresponding author at: Department of Bioengineering, University of Pittsburgh, PA, USA.
** Corresponding author at: The Center for the Neural Basis of Cognition, University of Pittsburgh, PA, USA.
E-mail addresses: sdm63@pitt.edu (S.D. McKeon), lunab@upmc.edu (B. Luna).
[1] Lead Contact

https://doi.org/10.1016/j.dcn.2024.101373
Received 12 February 2024; Received in revised form 1 April 2024; Accepted 2 April 2024
Available online 3 April 2024

glutamate/GABA balance across frontal cortex (Larsen et al., 2022; Perica et al., 2022). These findings correspond with an fMRI GABAergic benzodiazepine challenge study showing developmental increases in E/I balance (i.e. a decrease in the E/I Ratio) into adulthood in association cortices including PFC (Larsen et al., 2022; Perica et al., 2022). The implications of changes in E/I balance at the level of in vivo neural activity, however, remain poorly understood.

Both oscillatory and non-oscillatory frequency-specific activity have the potential to inform the neural functional consequences of changes in E/I balance. Synaptic interactions between PV interneurons and pyramidal neurons contribute to the regulation of E/I balance and the production of oscillatory activity, including high-frequency oscillations in the gamma band (30–70 Hz) thought to contribute to cognitive control (Tada et al., 2020). Oscillatory activity is measurable through electroencephalogram (EEG), which provides a non-invasive measure of post-synaptic cortical pyramidal neuron function of the cortical surface. Shifts in oscillatory activity may reflect structural and functional maturation, including the refinement of cortical circuitry, synaptic pruning, myelination, and alterations in E/I circuits (Hill et al., 2022; Uhlhaas et al., 2010). However, recent EEG work has demonstrated the importance of accounting for not only the oscillatory periodic activity, but the broadband background aperiodic activity. Aperiodic activity has previously been regarded as "noise" and physiologically irrelevant; though, recent work has shown that this non-cyclical activity reflects neuronal population spiking (Manning et al., 2009; Miller et al., 2012) and may be modulated by task-performance (Donoghue et al., 2020a; Podvalny et al., 2015). Importantly, it has been found to correspond with states of fluctuating E/I balance in rodent models (Donoghue et al., 2020a; Gao et al., 2017), and has been shown to be altered in neurological and psychiatric disease states (Hill et al., 2022; Molina et al., 2020; Ostlund et al., 2021; Robertson et al., 2019; Wilkinson and Nelson, 2021). This aperiodic activity has been proposed to be measurable by the slope of the power spectral density (PSD) as a function of frequency, that is, how power drops from low to high frequency bands. Previous work has demonstrated this effect by showing that local field potential (LFP) power in neuronal circuits is inversely related to frequency, following a 1/f distribution (Hill et al., 2022; Donoghue et al., 2020a; Buzsáki et al., 2012) and thought to be representative of the low-pass frequency filtering property of dendrites (Buzsáki et al., 2012; Lindén et al., 2010; Gold et al., 2006; Pettersen et al., 2008). Furthermore, large scale network mechanisms may also contribute to the 1/f power distribution, as networks with faster time constants, such as excitatory AMPA, have constant power at lower frequencies until they quickly decay, whereas inhibitory GABA currents have slower time constants at higher frequencies and thus decay more slowly as a function of frequency (Donoghue et al., 2020a; Gao et al., 2017), which when taken together, creates the 1/f like slope across broadband frequencies. These results suggest that E/I balance can affect PSD slope: when excitatory activity is greater than inhibitory activity, the 1/f slope will be lower (flatter), whereas it will be larger (steeper) when inhibitory activity is greater than excitatory activity (Donoghue et al., 2020a), suggesting the possibility that E/I balance is reflected in the steepness of the PSD slope. Spectral parameterization (specparam), formally known as Fitting Oscillations and 1/f (FOOOF), protocol derives the 1/f spectral slope (referred to as the aperiodic exponent) and an offset (Donoghue et al., 2020a). The steepness of the slope (i.e., the exponent) has been previously linked to shifts in the E/I balance (Donoghue et al., 2020a; Gao et al., 2017; Molina et al., 2020; Ostlund et al., 2021; Robertson et al., 2019; Zhang et al., 2011; Mamiya et al., 2021; Voytek et al., 2015), reductions of which reflect shifts toward excitatory activity relative to inhibitory, while increases in the exponent reflect shifts toward inhibitory activity (Donoghue et al., 2020a; Gao et al., 2017). Independently, the PSD offset is thought to reflect broadband shifts in power (Donoghue et al., 2020a), reflecting levels of neuronal population spiking (Manning et al., 2009; Miller et al., 2014). Electrocorticogram (ECoG) recordings from macaques (Gao et al., 2017) and human EEG studies (Waschke et al., 2021), have provided empirical support for the specparam protocol, showing that sedation by propofol a general anesthetic that modulates $GABA_A$ receptors and effectively decreases the global E/I ratio (Peduto et al., 1991), resulted in steepening of the power spectral density (PSD) slope (Gao et al., 2017; Waschke et al., 2021). Additional pharmacological work using MK-801, a NMDAR antagonists (Gonzalez-Burgos et al., 2023), known to down regulate inhibition, Diazepam, a $GABA_A$ R modulator (Gonzalez-Burgos et al., 2023; Salvatore et al., 2024), known to increase inhibition, and xenon, a NMDAR antagonist (Colombo et al., 2019), all demonstrated a steepening of the aperiodic slope. Interestingly, ketamine, known to down regulate inhibition and therefore increase excitation, showed a slight steepening of the aperiodic slope (Colombo et al., 2019), and a flattening in another study (Waschke et al., 2021). An additional study used Designer Receptors Exclusively Activated by Designer Drugs (DREADDs) to suppress the activity of PV interneurons, moving the activity toward excitation (Salvatore et al., 2024). However, they found the circuit disinhibition increased the E/I balance, contrary to their hypothesis (Salvatore et al., 2024). Ultimately, both low E/I due to barbiturates or propofol or high E/I as demonstrated by xenon or DREADDs, can lead to a steepening of the aperiodic slope, highlighting the need for further investigation into how the excitation inhibition circuitry reflects onto the aperiodic component.

Aperiodic activity has also been associated with behavioral performance across a variety of cognitive tasks (Donoghue et al., 2020a; Podvalny et al., 2015; Ouyang et al., 2020), including a reduction in the aperiodic exponent during visuomotor and object recognition tasks relative to baseline (Podvalny et al., 2015), indicating greater predominance of excitatory activity during task as compared to baseline. Further, developmental changes in aperiodic activity have been previously demonstrated, and occur simultaneously with developmental improvements in cognition during adolescence. From early childhood to young adulthood, there is a flattening of the aperiodic exponent and a reduction in offset, potentially reflecting an increase in the E/I balance (Hill et al., 2022; McSweeney et al., 2021; Tröndle et al., 2022; Cellier et al., 2021). Age-related changes in visual cortical 1/f spectral slopes have also been found to mediate age-related performance in visual working memory tasks for both younger (20–30yo) and older (60–70yo) adults (Voytek et al., 2015). Given compelling evidence for developmental changes in aperiodic activity, a next step is to understand the other neurobiological indicators of age-related E/I shifts to build models of possible mechanisms underlying maturation.

In this study, we collected a large, multimodal, longitudinal dataset including EEG as well as 7 T Magnetic Resonance Spectroscopic Imaging (MRSI). We assessed developmental changes in aperiodic activity in DLPFC as measured by EEG and investigated their association with our initial MRSI findings showing age-related increases in Glu/GABA balance in DLPFC through adolescence (Perica et al., 2022) in the same 10–32-year-old participants. We hypothesized that aperiodic activity would decrease through adolescence as Glu/GABA balance increased into adulthood (Larsen et al., 2022). In line with this hypothesis, we found strong correspondence between decreases in both offset and exponent through adolescence and increasing Glu/GABA balance into adulthood. Finally, we show how EEG- and MRSI- derived measures of E/I balance are associated with behavioral improvements in the latency of working memory responses as measured by the Memory Guided Saccade task. Taken together, this study provides *in vivo* multilevel validation for unprecedented plasticity in PFC through adolescence supporting cognitive development.

2. Methods

2.1. Participants

Data was collected on 164 participants (87 assigned female at birth), between 10 and 32 years of age. Participants were recruited as part of an

accelerated cohort design with up to 3 visits at approximately 18mo intervals. Each time point consisted of three visits: a behavioral (in-lab) session, a 7 T MRI scan, and an EEG session, typically occurring on different days within 1–2 weeks, for a total of 347 visits. Following data quality control and exclusion criteria, as described below, the final dataset included 283 sessions (Figure S1). Participants were recruited from the greater Pittsburgh area and were excluded if they had a history of loss of consciousness due to a head injury, non-correctable vision problems, learning disabilities, a history of substance abuse, or a history of major psychiatric or neurologic conditions in themselves or a first-degree relative. Patients were also excluded if any MRI contradictions were reported, including but not limited to, non-removable metal in their body. Participants or the parents of minors gave informed consent with those under 18 years of age providing assent. Participants received payment for their participation. All experimental procedures were approved by the University of Pittsburgh Institutional Review Board and complied with the Code of Ethics of the World Medical Association (Declaration of Helsinki, 1964).

2.2. Data acquisition and preprocessing

2.2.1. Electrophysiological (EEG) data

Concurrent EOG (electrooculogram) and high-impedance EEG was recorded using a Biosemi ActiveTwo 64-channel EEG system located in the PWPIC Psychophysiology Laboratory. EEG sessions were conducted in an electromagnetically shielded room while stimuli were presented by a computer approximately 80 cm away from participants. Resting state data was collected from four eyes open and eyes closed conditions, each lasting one minute and alternating between conditions. Initial data was sampled at 1024 Hz and resampled at 150 Hz during preprocessing. Scalp electrodes were referenced to external electrodes corresponding to the mastoids due to its proximity to the scalp and low signal recording. An initial bandpass filter was set to 0.5 – 90 Hz. Data were preprocessed using a revised processing pipeline compatible with EEGLAB (Delorme and Makeig, 2004), which removed flatline channels (maximum tolerated flatline duration: 8 seconds), low-frequency drifts, noisy channels (defined as more than 5 standard deviations from the average channel signal), short spontaneous bursts, and incomplete segments of data. Deleted channels were replaced with interpolated data from surrounding electrodes. The resulting data was referenced to the average reference. As a final preprocessing step, independent component analysis (ICA) was performed to identify eye-blink artifacts and remove their contribution to the data.

2.2.2. Magnetic resonance spectroscopy

MRSI methods have been previously reported in Perica et al. (2022). Briefly, data were acquired at the University of Pittsburgh Medical Center Magnetic Resonance Research Center using a Siemens 7 T scanner. Structural images were acquired using an MP2RAGE sequence (1 mm isotropic resolution, TR/TE/flip angle 1/ flip angle 2: 6000 ms/2.47 ms/4^0/5^0). MRSI including GABA and glutamate were acquired using a J-refocused spectroscopic imaging sequence (TE/TR = 2 ×17/1500 ms) and water suppression was performed using a broad band semi-selective refocusing pulse and frequency selective inversion recovery (Pan et al., 2010). Radiofrequency (RF) based outer volume suppression was used to minimize interference in the signal from extracerebral tissue (Hetherington et al., 2010). An 8 × 2 ^{1}H transceiver array using 8 independent RF channels was used to acquire data. High order shimming was used to optimize homogeneity of the B_0 magnetic field. The 2D CSI oblique axial slice was acquired with conventional rectangular phase encoding of 24 × 24 over a FOV of 216 × 216 mm (10 mm thick, 0.9 ×0.9 ×1.0 cm nominal resolution), and was positioned to include Brodmann Area 9 and pass through the thalamus.

2.2.3. Memory guided saccade task

Participants performed a memory guided saccade (MGS) task to assess working memory (see Figure S2) during the EEG session. The trial began with fixation to a blue cross for 1 sec. The participant was then presented with a peripheral cue with a surrounding scene picture to be used in a different study, in an unknown location along the horizontal midline (12.5 or 22.2 degrees from central fixation to left or right of center), where they performed a visually guided saccade (VGS) to the target and maintained fixation. Once the cue disappeared, the participant returned their gaze to the central fixation point and fixated for a variable delay epoch (6–10 sec) during which they were to maintain the location of the peripheral target in working memory. Once the central fixation disappeared the participant performed a memory guided saccade to the recalled location of the previous target. The trial ended when participants were presented with a white fixation cross that served as the ITI (1.5–15 sec). Participants performed 3 runs of the MGS task, each containing 20 trials.

Task performance was assessed based on horizontal electrooculogram (hEOG) channels recorded from facial muscles (see acquisition details below). At the start of the session, participants performed a calibration procedure in which they fixated a series of 20 dots sequentially, positioned along the horizontal midline and spanning the width of the screen. These were used to generate a calibration curve relating hEOG voltage to horizontal screen position. Eye position during the MGS task was used to derive output measures using this calibration data by aligning hEOG signals to different stimulus triggers. These were used to calculate VGS & MGS response latencies, as the time difference between the beginning of the recall epoch and the initiation of the VGS and MGS eye movements respectively, and saccadic accuracy, measured as the closest stable fixation point during the recall period to the fixated location during the initial visually guided fixation epoch.

2.2.4. Spatial span task

Participants preformed the Spatial Span Test from the Cambridge Neuropsychological Test Automated Battery (CANTAB) (De Luca et al., 2003) that assesses working memory capacity. During the task white squares appear on the screen, some of which will briefly change color in a variable sequence. The participant must select the boxes that changed color in the same order that they were presented. The number of boxes in the sequences begins with two and increases, after each successful trial, to a maximum of nine. The outcome measure was the maximum sequence length the participant successful completed, between 2 and 9.

2.3. Data analysis

2.3.1. EEG analyses

Power spectral density (PSD) was calculated separately for each participant and electrode, corresponding to the left and right DLPFC (Right: F4, F6, F8; Left: F3, F5, F7), across the continuous resting state EEG using Welch's method implemented in MATLAB (2 s Hamming window, 50% overlap). The Fitting Oscillations and One Over *f* (FOOOF) python toolbox (version 1.0.0; https://fooof-tools.github.io/fooof/), now known as Spectral Parametrization (specparam), was used to characterize the PSD as a combination of an aperiodic component with overlying period components, or oscillations (Donoghue et al., 2020a) (see Fig. 1A). Oscillations were characterized as frequency regions with power above the aperiodic component, modeled as a Gaussian, and are referred to as 'peaks'. The aperiodic component $L(f)$ was extracted from the 1–50 Hz frequency range of each power spectrum (*aperiodic_mode* = 'fixed', *peak_width_limits* = [0.5, 12], min _peak_height = 0, *peak_threshold* = 2, max _n_peaks = 4, default settings otherwise), and is expressed as:

$$L(f) = b - \log[f^x],$$

with a constant offset b and the aperiodic exponent x. When the PSD is plotted on a log-log axis, the constant offset b refers to the y-intercept and the aperiodic exponent x corresponds to the slope of a line (see

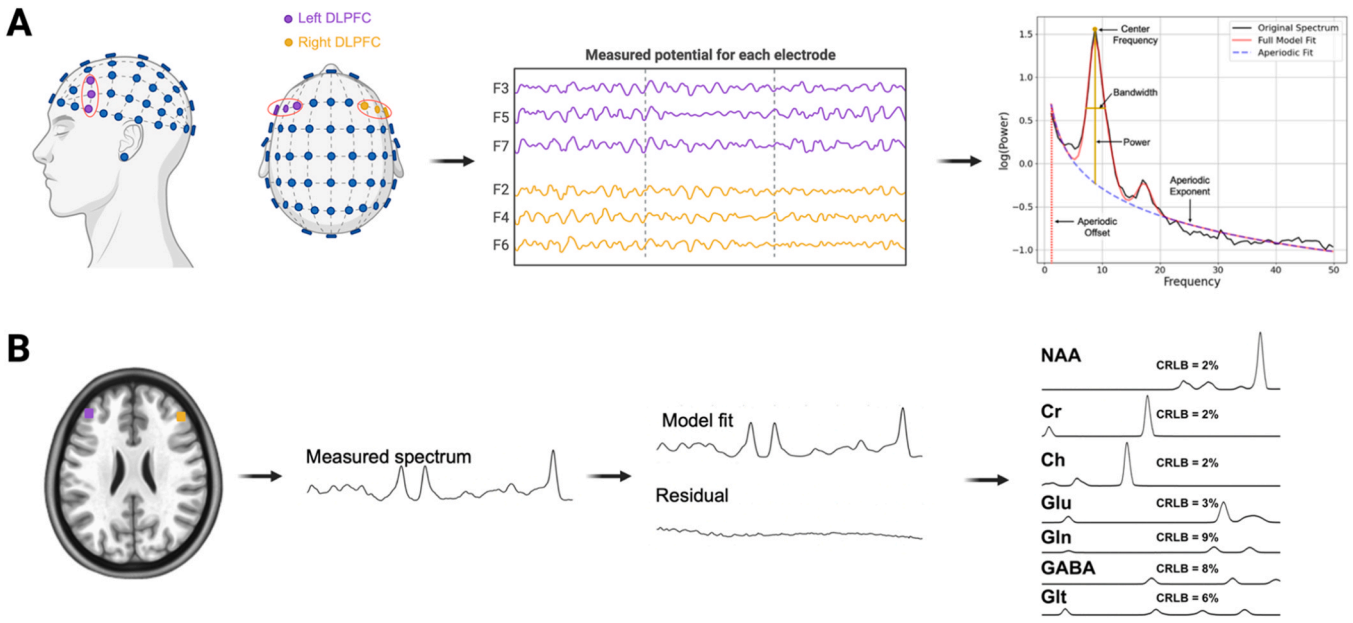

Fig. 1. Graphical representation of the methods. **A.** EEG acquisition from the electrodes corresponding to the left and right DLPFCs to decomposing the signal into the aperiodic component to extract the exponent and offset. **B.** MRSI methods from placement of the DLPFC ROIs to modeling fitting and extracting the GABA and Glutamate levels. Created with Biorender.com.

Fig. 1A). We used the 'fixed' setting as we did not expect a "knee" in the power spectrum. This assumption was supported upon visual inspection of each PSD. The average R^2 of the spectral fits was 0.98 for the eyes closed condition and 0.97 for the eyes open condition, reflecting good fits, while the average mean absolute error was 0.042 for eyes open and 0.05 for eyes closed. We have also included group mean spectra for our three age groups: 10–16, 17–22, and 23–30, as well as representative fits for each group from individual subjects (Figure S3).

2.3.2. MRS analyses

Analysis details have been previously reported in Perica et al. (2022) (Fig. 1B). LCModel was used to obtain estimates of individual metabolites (Provencher, 2001), including macromolecule components and 14 basis metabolite functions (N-acetylaspartate (NAA), N-acetylaspartylglutamate (NAAG), aspartate, lactate, creatine (Cre), γ-aminobutyric acid (GABA), glucose, glutamate (Glu), glutamine, glutathione, glycerophosphorylcholine (GPC), phosphorylcholine (PCh), myoinositol, and taurine), of which we focus on GABA and Glu for the purposes of this study.

A 2D CSI oblique axial slice was acquired, as outlined in Perica et al. (2022), to ensure that the dorsolateral prefrontal cortex (DLPFC) was included and angled to pass through the thalamus. Regions of interest included right and left DLPFC due to its role in working memory. Data quality exclusion was performed at the ROI level. All spectra and model fit outputs were visually inspected and used as first-pass exclusion criteria, followed by Cramer-Rao Lower Bound (CRLB) > 10 for the three major metabolite peaks (GPC/Cho, NAA/NAAG, and Cr), and CRLB > 20 for glutamate and GABA. All glutamate and GABA levels are given as ratios to creatine (Cr). Metabolite levels were corrected for fractional gray matter within the voxel as well as date to control for any changes in scanner precision over time, while controlling for age. Glu/GABA ratio was calculated by creating a ratio of Glu/Cr to GABA/Cr. Glu-GABA asymmetry was calculated by taking the absolute value residual of the linear model of the association between Glu/Cr and GABA/Cr. We used a Kolmogorov-Smirvov test to assess the normality of the Glu-GABA asymmetry. The sample was found to be non-normal as indicated by a p- value = 4.39e-07. Thus, the square root of the data was taken, resulting in a new p-value of 0.052, allowing us to conclude that the data follows a standard normal distribution. A threshold of 2 standard deviations from the mean was used to exclude statistical outliers.

2.3.3. Behavioral analyses

To examine age-related effects in behavioral measures, including accuracy and response latency, generalized additive mixed models (GAMMs) were implemented using the R package mgcv (Wood, 2017). Preliminary outlier detection was conducted on a trial level basis. Express saccades of less than 100 ms, believed to be primarily driven by subcortical systems (Luna et al., 2008), were excluded. Position error measures greater than 23 degrees from the target were excluded as implausible since they exceeded the width of the screen. The remaining trials for each participant were combined, creating average performance measures and trial-by-trial variability measures for each participant. Finally, for group level analyses, outlier detection was performed, excluding participants more than +/-2 SDs away from the mean. A separate model was performed for each of the behavioral measurements: MGS accuracy, MGS latency, as well as the trial-by-trial variability of each measure. To correct for multiple comparisons between the four behavioral measures, Bonferroni correction was employed which resulted in a corrected alpha of.0125 (p =.05/4 =.0125). For all behavioral measures showing significant age-related effects, we performed analyses to identify periods of significant age-related change. To do so, a posterior simulation was performed on the first derivative of the GAM model fits. Consistent with previous work (Wood, 2017; Simmonds et al., 2014; Calabro et al., 2020), 10000 simulated GAM fits and their derivatives (generated at age intervals of 0.1 years) were computed from a multivariate normal distribution; vector means and covariance of which corresponded to the fitted GAM parameters. Confidence intervals (95%) were generated from the resulting derivatives. The periods of age-related growth were derived from the ages corresponding to when the confidence interval did not include zero ($p < 0.05$).

For the spatial span task, we used generalized additive mixed models (GAMMs), implemented using the R package mgcv (Wood, 2017), to assess age-related effects in maximum sequence length. We then performed analysis to identify specific periods of significant age-related change. The same method was used for Spatial Span as described above.

2.4. Statistical analyses

2.4.1. Characterizing age-related trends in 1/f aperiodic activity

To assess developmental trajectories of aperiodic activity, we implemented GAMMs on aperiodic parameter (exponent and offset), including random intercepts estimated for each participant. Regression splines were implemented (4 degrees of freedom) to assess linear and non-linear effects (Wood, 2017, 2013). We first tested for a main effect of age on aperiodic parameter while controlling for hemisphere (either 'right' or 'left' DLPFC) and condition (eyes open or eyes closed during resting state), seen in Model 1 in Supplement. We additionally tested for age-by-hemisphere interactions while controlling for condition (Supplement Model 2), and age-by-condition interactions while controlling for region (Supplement Model 3). Correlations between the exponent and the offset, for both the eyes open and eyes closed conditions were calculated using Pearson correlations.

2.4.2. Characterizing age-related trends in MRSI-derived metabolite levels

To assess age-related change in the Glu/GABA ratio and the Glu-GABA asymmetry in right and left DLPFC, we used GAMM models, including random intercepts estimated for each participant. Regression splines were implemented (4 degrees of freedom) to assess linear and non-linear effects (Wood, 2017, 2013). We first tested for a main effect of age on the MRS measure while controlling for hemisphere (either 'right' or 'left' DLPFC), and perfect grey matter from the MRI voxel (Supplement Model 4). We additionally tested for age-by-hemisphere interactions while controlling for fraction of grey matter (Supplement Model 5). For further analysis, fraction of gray matter in the voxel was residualized out of MRSI estimates to control for the effect of gray matter.

2.4.3. Characterizing the relationship between 1/f aperiodic activity and MRS

We next investigated the relationship between the individual aperiodic parameters (exponent and offset) on MRSI-derived measures of the Glu-GABA asymmetry using linear mixed effect models (lmer function, lme4 package in Rstudio (Bates et al., 2015)). Using AIC, we determined an inverse age (age^{-1}) model was more appropriate for both the exponent vs MRS and offset vs MRS associations (Table S1), thus each model controlled for inverse age. We first tested for significant main effects of the MRS measure on the aperiodic parameter while controlling for age^{-1}, condition (eyes open or eyes closed), and hemisphere (left or right DLPFC) (Supplement Model 6). We additionally tested for MRS-by-age^{-1} interactions while controlling for hemisphere and condition (Supplement Model 7). To account for the four aperiodic measures, Bonferroni correction was used for multiple comparisons at $p_{bonferroni} = 0.012$.

To test for relationships between the age-related differences in the MRS measures and age- related differences in the aperiodic measures, mediation analyses were implemented using the R package *mediation (*Tingley et al., 2014*)*. Unstandardized indirect effects were computed for each of 1000 bootstrapped samples, and the 95% confidence interval was computed by determining the indirect effects at the 2.5th and 97.5th percentiles.

2.4.4. Characterizing the relationship between 1/f aperiodic activity and behavior

To assess associations between 1/f aperiodic parameters (exponent and offset), MGS behavioral measures (accuracy, accuracy variability, response latency, and response latency variability), and spatial span measure (maximum length of sequence), we used linear mixed effect models (lmer function, lme4 package in Rstudio (Bates et al., 2015)). Using AIC, we determined an inverse age (age^{-1}) model was more appropriate for both the exponent vs behavior and offset vs behavior associations (Table S2). We first tested for significant main effects of the behavioral measure on the aperiodic parameter while controlling for inverse age (age^{-1}), condition (eyes open or eyes closed), and hemisphere (left of right DLPFC) (Supplement Model 8). We additionally tested for behavior-by-inverse age interactions while controlling for condition and hemisphere (Supplement Model 9). Bonferroni correction was used for multiple comparisons.

2.4.5. Characterizing the relationship between MRS and behavior

To assess associations between MRS measures (asymmetry) and MGS behavioral measures (accuracy, accuracy variability, response latency, and response latency variability), and spatial span measure (maximum length of sequence), we used linear mixed effect models (lmer function, lme4 package in Rstudio (Bates et al., 2015)). Using AIC, we determined an inverse age model was best for the glutamate, GABA, and asymmetry vs behavioral associations (Table S2). We first tested for significant main effects of the behavioral measure on the aperiodic parameter while controlling for age^{-1} and hemisphere (left of right DLPFC) (Supplement Model 10). We additionally tested for behavior-by-age interactions while controlling hemisphere (Supplement Model 11). Bonferroni correction was used for multiple comparisons.

3. Results

3.1. Working memory performance improves across adolescence

Consistent with our prior findings using the MGS task (Luna et al., 2008; Montez et al., 2017, 2019), behavioral performance improved with age for all MGS metrics including increased accuracy ($F = 38.19$, $p = <2e\text{-}16$; Figure S4A), decreased response latency ($F = 17.91$, $p = <2e\text{-}16$; Figure S4B), and decreased trial-to-trial variability in both accuracy ($F = 29.1$, $p = <2e\text{-}16$; Figure S4C) and response latency ($F = 52.04$, $p = <2e\text{-}16$; Figure S4.D). Significant developmental improvements were found throughout adolescence (11–24 years of age) for MGS accuracy and between 10 and 24 years of age for trial-by-trial variability for MGS accuracy (Figure S4.A and Figure S4C). MGS latency showed significant increases in adolescence (12–17 and 19–22 years of age, Figure S4B), while decreases in MGS variability in latency continued into the twenties (Figure S4D). Furthermore, working memory capacity also improved across adolescence via the Spatial Span task as seen in a significant increase in the maximum number of boxes presented in the sequence ($F = 11.35$, $p = 0.00035$; Figure S5). Significant developmental improvements were found between 10 and 17 years of age.

3.2. Glutamate GABA asymmetry decreases through adolescence

As in our prior cross-sectional study (Perica et al., 2022), glutamate showed age-related decreases across adolescence ($F = 4.70$, $p = 0.04$; Fig. 2A), while there were no significant age effects with GABA ($F = 0.50$, $p = 0.48$; Fig. 2B). As previously, we assessed Glu/GABA balance by assessing asymmetry, an individual-level measure of the correlation between glutamate and GABA which was defined as the absolute difference in age-adjusted Glu and GABA levels (see methods), and was found to significantly decrease with age ($F = 13.58$, $p = 0.0003$; Fig. 2D). As expected, due to greater inter-subject variability at younger ages in Glu and GABA (Fig. 2E) undermining the ability to assess age related changes in balance (Perica et al., 2022), the ratio was not associated with age ($F = 4.96$, $p = 0.05$; Fig. 2C). Thus, analyses going forward utilized the Glu-GABA asymmetry measure. Additional statistics regarding main effects of hemisphere and age-by-hemisphere interactions can be found in the supplement (Figure S5).

3.3. 1/f aperiodic activity decreases through adolescence

To assess changes in signal processing characteristics through adolescence, each specparam model parameter was tested for associations with age. For the aperiodic EEG exponent measure, which captures the steepness of the relationship between power and frequency, we

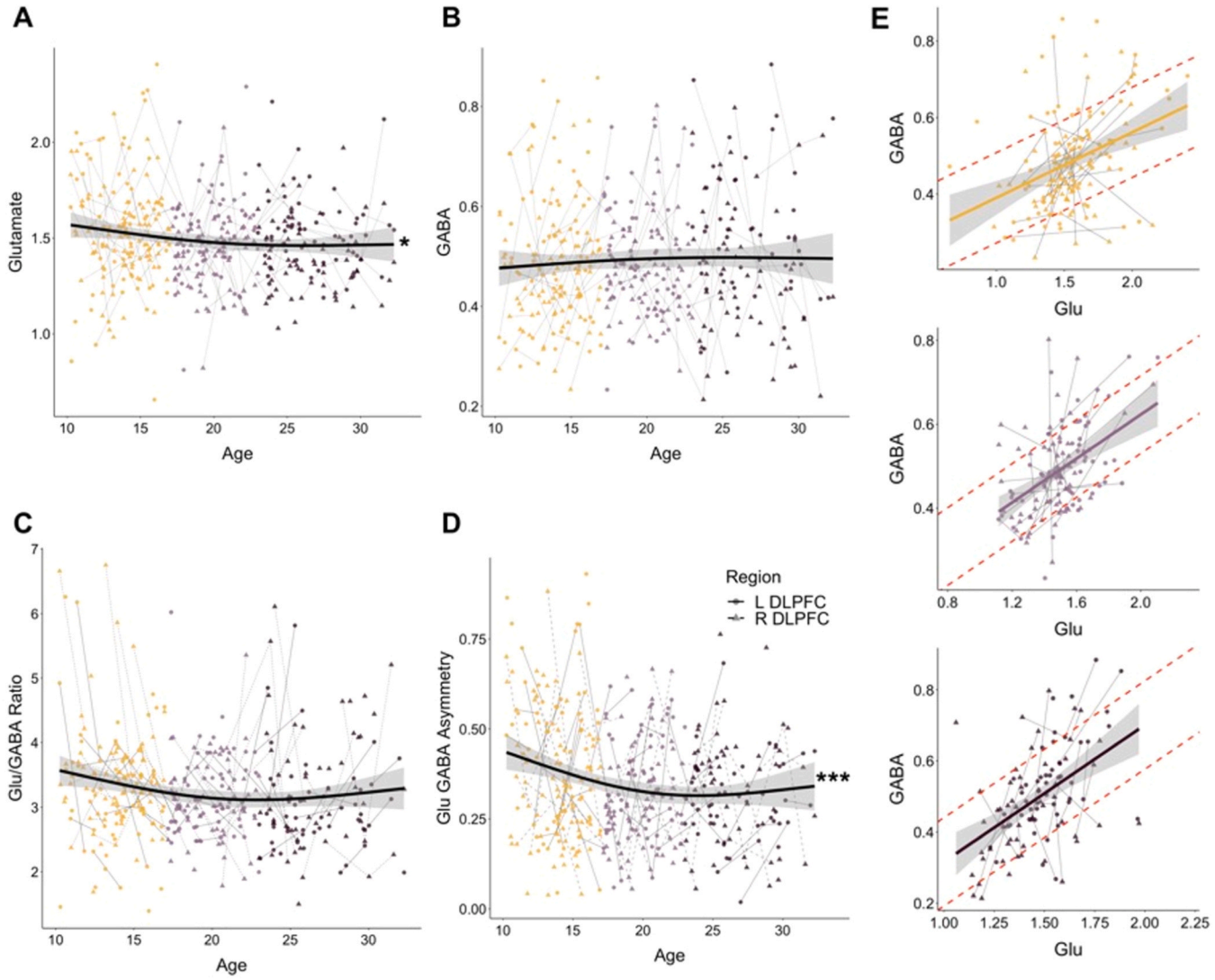

Fig. 2. MRSI derived metabolite levels across adolescence. A. Glutamate vs age across adolescence. B. GABA vs age across adolescence C. Glu/GABA Ratio vs age across adolescence. D. Glutamate GABA asymmetry vs age. E. Top: GABA vs Glu for the 10–16-year-old age group. Middle: GABA vs Glu for the 17–22-year-old age group. Bottom: GABA vs Glu for the 23 and up age group. Red lines represent ± 1 SD away from the smoothed line to help visualize the increased variance in the youngest age group. (* $p < 0.01$; ** $p < 0.001$; *** $p < 0.0001$).

found significant age-related decreases ($F = 61.85$, $p < 0.0001$; Fig. 3A). The aperiodic offset, which captures the overall power independent of frequency, was also found to significantly decrease with age ($F = 237.1$, $p < 0.0001$; Fig. 3B). The PSDs for the various age groups (10–16; 17–22; 23+) can be seen in Fig. 3C. Furthermore, group mean spectra and corresponding representative fits on individual subjects within an age group can be seen in Figure S3. The exponent and offset were highly correlated across both conditions ($r = 0.75$, $p < 2.2e\text{-}16$) (Figure S7C). Additional statistics including the effect of condition (eyes open vs eyes closed) and hemisphere (right vs left DLPFC) can be found in the Figure S7.

3.4. Associations between 1/f aperiodic activity and MRS

To characterize the functional associations of MRSI-derived metabolite levels, we next assessed associations between EEG-derived specparam measures and Glu-GABA asymmetry. All statistics were conducted controlling for inverse age and are reported in Table S3 with corrected *p*-values. The Glu-GABA asymmetry significantly increased with increasing aperiodic exponent ($\beta = 0.21$, $t = 3.91$, $p = 0.0002$; Fig. 4A) and offset ($\beta = 0.18$, $t = 3.25$, $p = 0.002$; Fig. 4B). To interrogate whether the effects of the Glu-GABA asymmetry on the aperiodic activity was driven by glutamate or GABA, we conducted post hoc analyses of these associations. Here, we found glutamate to significantly increase with increasing exponent ($\beta = 0.07$, $t = 2.14$, $p = 0.03$; Fig. 4C), and a trending increase with offset ($\beta = 0.06$, $t = 1.77$, $p = 0.08$; Fig. 4D). GABA did not have a significant association with either exponent ($\beta = 0.04$, $t = 0.71$, $p = 0.48$; Fig. 4E) nor offset ($\beta = 0.05$, $t = 0.64$, $p = 0.40$; Fig. 4F). Knowing how correlated the aperiodic exponent and offset are, we investigated whether the associations between the exponent and Glu-GABA asymmetry was still significant when controlling for the offset, and visa-versa if the offset and asymmetry was still significant when controlling for exponent. Interestingly, we find that the exponent and Glu-GABA asymmetry are still significantly associated when controlling for offset ($\beta = 0.08$, $t = 2.10$, $p = 0.04$) but offset is no longer significantly associated with Glu-GABA asymmetry when controlling for exponent ($\beta = 0.04$, $t = 1.13$, $p = 0.26$).

To further interrogate the contribution of metabolite levels to the generation of aperiodic activity, we performed mediation analyses for MRSI measures that showed significant associations with aperiodic EEG. Glu-GABA asymmetry was a significant mediator of age-related changes in the specparam exponent parameter (ACME: −0.0009, 95% CI [-0.002,

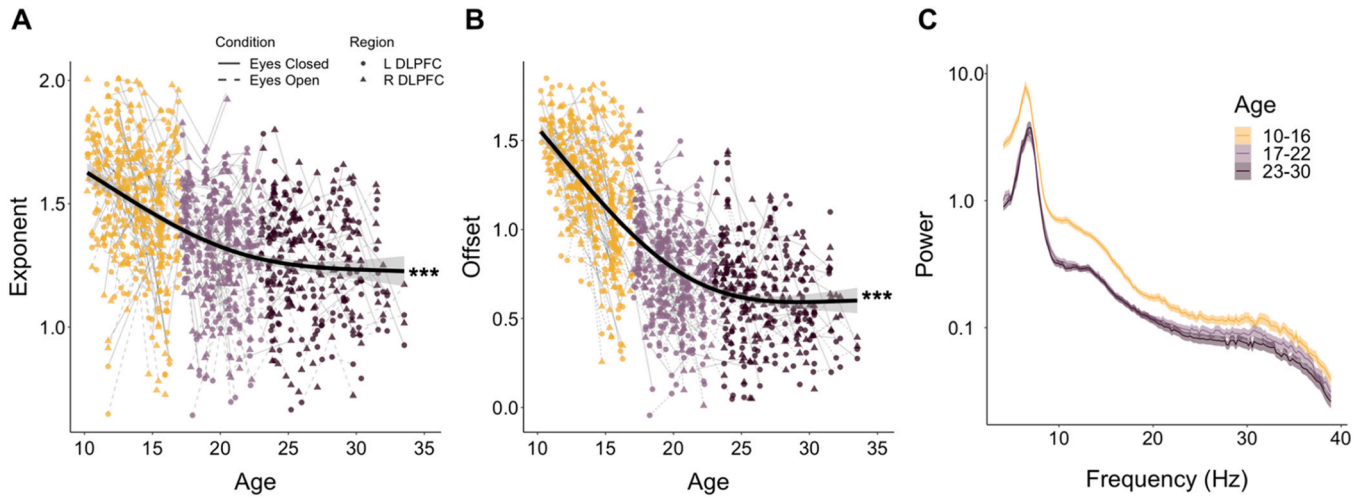

Fig. 3. Aperiodic activity of EEG during resting state. **A.** Exponent across adolescence across both eyes closed and eyes open conditions. **B.** Offset across adolescence across both eyes closed and eyes open. **C.** PSDs for the 10–16-year-old age group (gold), the 17–22-year-old age group (plum), and the 23+ age group (dark purple). (* $p < 0.01$; ** $p < 0.001$; *** $p < 0.0001$).

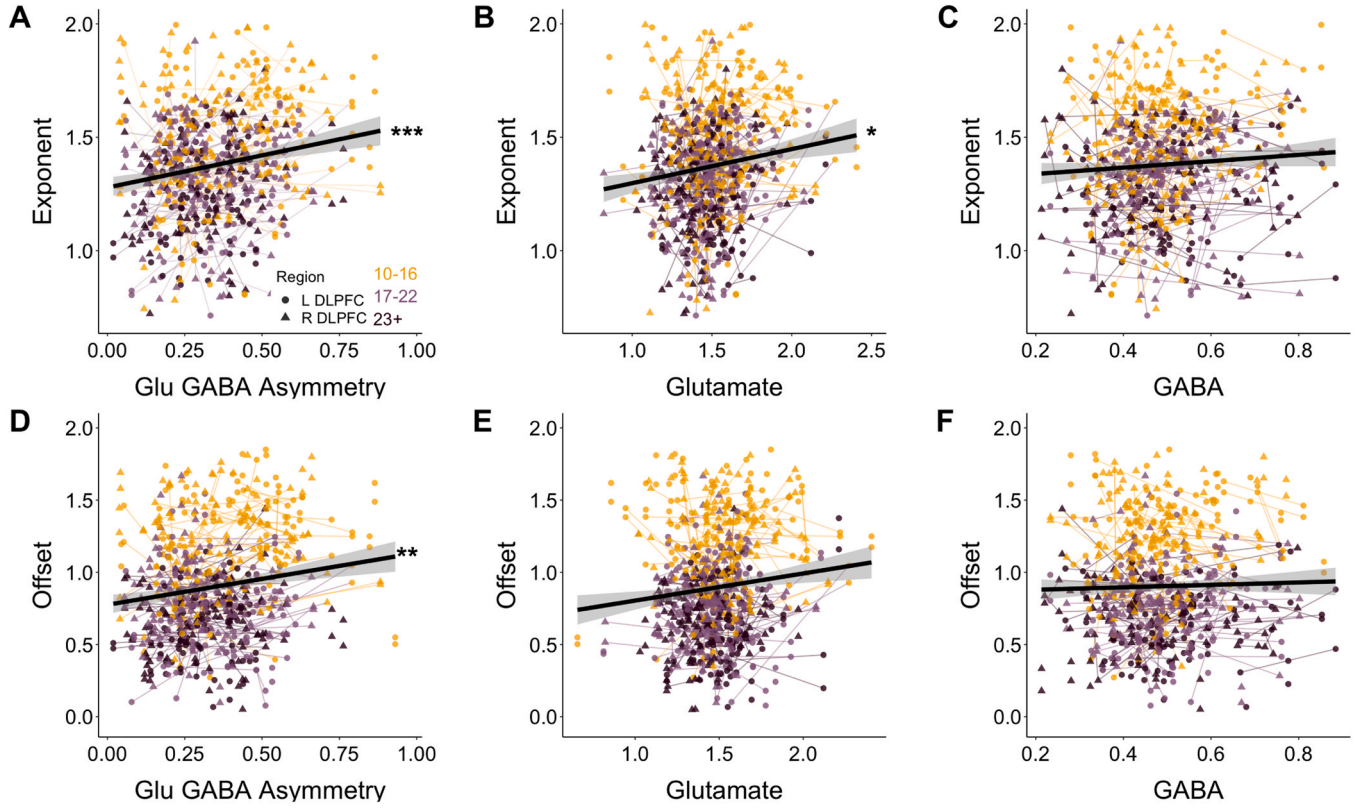

Fig. 4. Aperiodic EEG activity associations with MRS measures. Participants are grouped according to age; 10–16 (gold), 17–22 (light purple) and 23+ (dark purple). **A.** Exponent vs Glu-GABA asymmetry. **B.** Exponent vs Glutamate **C.** Exponent vs GABA **D.** Offset vs Glu-GABA asymmetry **E.** Offset vs Glutamate **F.** Offset vs GABA. (* $p < 0.01$; ** $p < 0.001$; *** $p < 0.0001$).

0.00], $p = 0.006$; Fig. 5A) as well as the offset parameter (ACME: −0.0009, 95% CI [-0.002, 0.00], $p = 0.014$; Fig. 5B). Glutamate was found to significantly mediate age-related changes in exponent (ACME: −0.00043, 95% CI [-0.001, 0.00], $p = 0.036$; Fig. 5C) but did not mediate age-related changes in offset (ACME: −0.0003, 95% CI [-0.001, 0.00], $p = 0.13$; Fig. 5D).

3.5. Steepened aperiodic activity is associated with improved working memory performance

To characterize the functional significance of our age-related changes in 1/f aperiodic activity, we assessed their relationship with our MGS working memory task, and the spatial span task. All associations and their statistics can be found in Table S4. and Figure S8. Exponent showed a trend-level positive association with MGS response latency (b = −0.63, t = −2.44 $p = 0.06$; Fig. 6A), and offset was

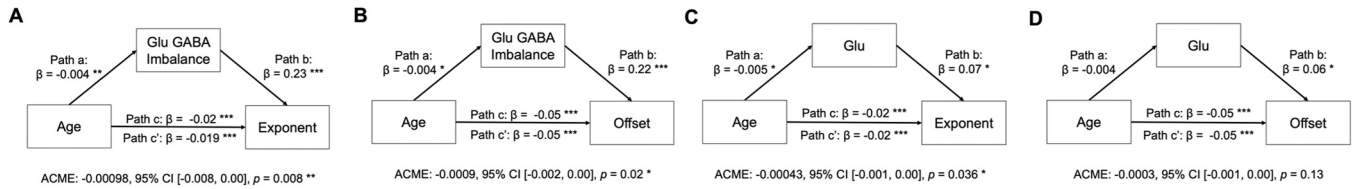

Fig. 5. Mediation Analyses. **A.** Glu-GABA asymmetry mediation on age-related exponent. **B.** Glu-GABA asymmetry mediation on age-related offset. Glutamate mediation on age-related changes on offset **C.** Glutamate mediation on age-related changes on exponent **D.** Glutamate mediation on age-related changes on offset.

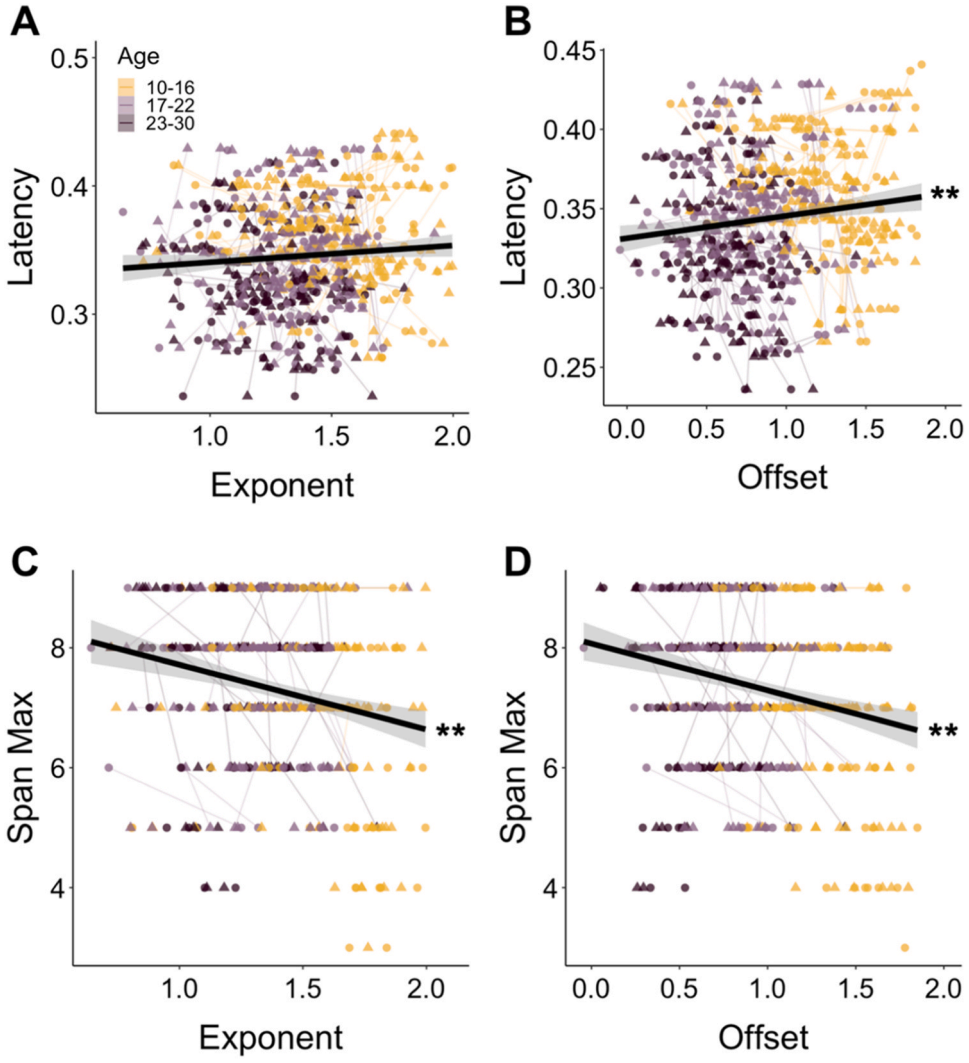

Fig. 6. Aperiodic EEG activity associations with behavioral measures. Participants are grouped according to age; 10–16 (gold), 17–22 (light purple) and 23+ (dark purple). **A.** Exponent vs MGS response latency **B.** Offset vs MGS response latency **C.** Exponent vs Spatial span max sequence length **D.** Offset vs Spatial span max sequence length. (** $p < 0.001$).

significantly associated with increased response latency ($b = -1.04$, $t = -3.60$, $p = 0.001$; Fig. 6B). Furthermore, a flatter exponent ($\beta = -0.04$, $t = -3.09$, $p = 0.002$; Fig. 6C) and offset ($\beta = -0.04$, $t = -3.12$, $p = 0.002$; Fig. 6D) were associated with increased maximum sequence lengths indicating improved spatial span performance.

To characterize the functional significance of our age-related changes in our MRS measures, we assessed their relationship with our MGS working memory task and the spatial span task. All associations and their statistics can be found in Table S4 and Figure S8. Glu-GABA asymmetry had no relationship with response latency ($b = -0.01$, $t = -0.06$, $p = 1$; Fig. 7A). There was a significant latency-by-inverse age interaction on Glu-GABA asymmetry ($b = 34.29$, $t = 3.28$, $p = 0.004$). To interrogate whether behavior may be driven by glutamate or GABA, we conducted post hoc analyses of these associations. Here we found increasing response latency was associated with increasing glutamate ($b = 1.00$, $t = 3.55$, $p = 0.002$; Fig. 7B), but no association with GABA ($\beta = 0.00$, $t = -0.01$, $p = 1.00$; Fig. 7C).

4. Discussion

Using novel EEG and MRSI methods in a large, longitudinal, developmental dataset spanning adolescence through young adulthood, this study suggests an association between developmental changes in DLPFC glutamate and GABA and changes in EEG-based markers of neural

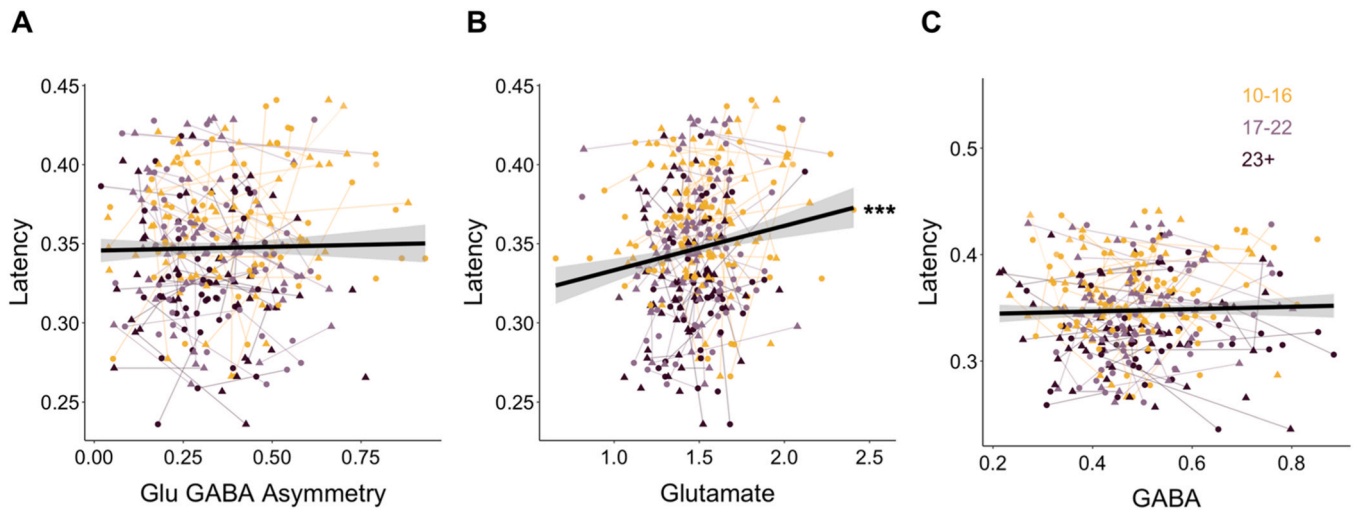

Fig. 7. MRSI associations with behavioral measures. Participants are grouped according to age; 10–16 (gold), 17–22 (light purple) and 23+ (dark purple). **A.** Glu-GABA asymmetry vs MGS response latency **B.** Glu vs MGS response latency **C.** GABA vs response latency (*** $p < 0.0001$).

excitatory and inhibitory activity. Consistent with previous reports (Hill et al., 2022; McSweeney et al., 2021; Tröndle et al., 2022; Cellier et al., 2021), we found age-related decreases in both the offset and exponent parameters of EEG-based aperiodic activity across both eyes open and eyes closed conditions. Furthermore, extending our prior cross-sectional findings, we found that balance between glutamate and GABA increased longitudinally through adolescence. Post-hoc analyses highlighted the developmental decreases in Glu-GABA asymmetry may be driven by significant age-related decreases in glutamate. Importantly, we found that Glu-GABA asymmetry was associated with the EEG-derived power spectrum slope (specparam exponent), and offset, with more asymmetry between glutamate and GABA being associated with steeper and higher power spectra. Interestingly, glutamate was found to significantly decrease with decreasing exponent (flatter slope), but only had a trending association with offset suggesting that age related decreases in E/I balance may be primarily underlined by increases in inhibitory function relative to excitatory function reflected in decreases in local field potentials more so than changes in neural spike rates. Furthermore, we found that Glu-GABA asymmetry mediated the association between age and aperiodic exponent and offset, while glutamate mediated the associations between age and aperiodic exponent, providing a neurobiological mechanistic link between age and aperiodic neural activity. To interrogate the developmental effects of E/I balance on behavior, we assessed working memory via two working memory tasks: the memory guided saccade (MGS) task and the CANTAB Spatial Span task. In line with prior findings (McKeon et al., 2023), we observed robust developmental improvements in working memory accuracy and latency (in the MGS task) and capacity (in the spatial span task). Interestingly, decreases in working memory latency were significantly associated with decreases in glutamate as well as decreases in the aperiodic offset, while working memory capacity was found to improve with decreasing offset and exponent. Taken together, these results suggest developmental shifts in the neurobiological mechanisms of excitation and inhibition, measurable through EEG and MRSI, may support the development of higher order cognitive functions across adolescence.

Previous work highlights the importance of interpreting neurophysiological recordings as a combination of periodic (oscillatory) and aperiodic components. Age-related differences in band specific power may thus arise in part due to a shift in the aperiodic slope (exponent) or intercept (offset) (Donoghue et al., 2020a). Our findings show that exponent and offset decrease with age during adolescence, largely in line with the extant literature, including prior findings of flatter 1/f slopes (exponent) and reduced offset values in older children compared to younger children (Hill et al., 2022; McSweeney et al., 2021; Tröndle et al., 2022; Cellier et al., 2021) (Fig. 3C). This result has been extended in adult populations, with exponent and offset decreasing across the lifespan (Voytek et al., 2015; Merkin et al., 2023). These results have been interpreted based on the hypothesized neurophysiological underpinnings of these measures. The spectral slope is thought to reflect the E/I balance via decays in local field potential (LFP) power constrained by faster decaying excitatory AMPA and slowly decaying inhibitory GABA currents (Buzsáki et al., 2012), with steeper slopes representing inhibitory activity dominating over excitatory (Donoghue et al., 2020a). In parallel, the amplitude of the spectra, assessed by the aperiodic offset parameter, is associated with neural spike rates (Waschke et al., 2021; Donoghue et al., 2020b), supported by intracranial LFP recordings that have shown increases in broadband LFP power associated with neuronal population spiking (Manning et al., 2009). Furthermore, recent work has associated the flattening of the aperiodic slope to a reduction in the autocorrelation of brain activity, allowing for more efficient information processing (He, 2014; He et al., 2019). Shifts in excitatory-inhibitory circuits, reflected by a change in the aperiodic model parameters, may thus reflect cortical maturation including refinement of cortical networks, synaptic pruning, myelination, and alterations in the E/I balance (Hill et al., 2022; Uhlhaas et al., 2010; De Bellis et al., 2001). Thus, our results showing robust reductions in aperiodic offset could be indicative of maturational decreases in overall spike rate of cortical neurons, while our results showing decreases in exponent suggest maturational increases in the E/I balance. It is worth noting that while the exponent and offset can vary independently, any change in exponent at a non-zero frequency will result in a change in offset as well, thus the high correlation of between exponent and offset is expected. However, a change in offset may be driven by a change in exponent, or E/I balance, and not necessarily a change in neural spiking.

In our previous work in a cross-sectional study we found increasing balance between glutamate and GABA across frontal regions, including DLPFC, through adolescence into adulthood (Perica et al., 2022). Here, we confirm these results in a longitudinal continuation of our cohort. Previous work has shown that structurally, excitatory and inhibitory synapses maintain a fairly constant ratio (Sahara et al., 2012), the location of which are regulated by changes in connectivity as a result of synaptic pruning (Sukenik et al., 2021). Functionally, E/I currents are thought to maintain balance via a "push-pull" mechanism, constantly blocking and activating excitatory and/or inhibitory receptors (Sukenik et al., 2021). Mice hippocampal cultures and modeling work has shown that for networks with a range of E/I fractions, ranging from 10% to 80% inhibitory neurons, the networks maintain stable neuronal activity (Sukenik et al., 2021). Developmental changes in E/I balance may

reflect an increase in "optimal" quantity of E and I activity that provides a state of low firing rates without hyper or hypo activity in response to stimuli. Developmentally, neural networks are trying to optimize processing given the specific cognitive demands and age, thus, age-related decreases in the Glu-GABA asymmetry across adolescence may be reflecting the optimization of the excitatory and inhibitory currents that result in balance. Furthermore, post-hoc analyses revealed decreases in glutamate across adolescence. Levels of Glu/Cr as measured by spectroscopy have been linked to PET-derived measures of synaptic density (Onwordi et al., 2021), suggesting that during adolescent development, synaptic pruning, which affects primarily excitatory synapses in prefrontal cortex (Petanjek et al., 2011), could lead to decreases in levels of glutamate and decreased neural population activity as indexed by offset. Studies that can make a more direct link between synaptic pruning and its modulation of excitatory activity are warranted.

Previous computational modeling (Donoghue et al., 2020a; Gao et al., 2017) and electrophysiology (Gao et al., 2017) work has found that the flattening of the aperiodic slope is indicative of the neural network favoring excitation over inhibition. However, recent work using pharmacological manipulation, has shown that modulating the E/I balance in either direction (increasing E relative to I or increasing I relative to E) via propofol (Colombo et al., 2019), diazepam (Gonzalez-Burgos et al., 2023; Salvatore et al., 2024), MK-801 (Gonzalez-Burgos et al., 2023), ketamine (Colombo et al., 2019), or xenon (Colombo et al., 2019), all steepen the aperiodic slope. Importantly, we found decreases in the Glu-GABA asymmetry did not only have a significant association with decreasing exponent (i.e., a flattening of the slope) and offset, but mediated the effects as well, demonstrating the functional significance of Glu-GABA coupling. Our results, in conjunction with the complex pharmacological manipulations on the E/I balance, suggests that the Glu-GABA asymmetry measure may be more indicative of the E/I balance, via the changes in correlation between excitatory and inhibitory neurons (Miller et al., 2009) and may support the notion that E/I balance may be inferred through the PSD slope exponent, providing important methodological backing to the specparam protocol using empirical longitudinal data and vice versa. Due to the high correlation between exponent and offset, it was not surprising that both measures were associated with Glu-GABA asymmetry, although exponent is considered to be a measure of E/I balance compared to offset that indicates neuronal population spiking. In addition, post-hoc analyses revealed associations between decreasing Glu/Cr and decreasing aperiodic exponent, as well as trends with decreasing offset. The associations with the exponent suggest that developmental decreases in Glu may be driving the decreases in Glu-GABA asymmetry, thus increasing the E/I balance which is consistent with a lower or flatter exponent. To further interrogate these associations, we tested the effect of the exponent and offset on Glu-GABA asymmetry while controlling for the other aperiodic parameter. This revealed that the association between Glu-GABA asymmetry and exponent remained significant, while offset did not, suggesting that the relationship with exponent may be more robust than offset and may be driving the observed associations. Our results correspond with known synaptic pruning of excitatory neurons in PFC through adolescence, which would result in decreases in Glu, decreased neural population activity as indexed by offset, as well as more efficient signal transmission across a full range of frequencies.

Using two working memory measures, the MGS and Spatial Span tasks, we assessed whether working memory was associated with our measures of E/I balance. DLPFC is a region that is known to be involved in visuo-spatial working memory (Goldman-Rakic, 1995), and exhibits a protracted developmental trajectory through adolescence (Gogtay et al., 2004). Both accuracy and latency, derived from the MGS task, are important but distinct components underlying overall executive function, with accuracy reflecting number of correct responses and latency reflecting the speed of information processing prior to making a response (Tervo-Clemmens et al., 2022; Ravindranath et al., 2022). Using the MGS task, we found significant associations between decreasing offset and decreasing response latency. While we did not find any associations between Glu-GABA asymmetry and accuracy or latency, post hoc analyses showed a significant negative relationship between response latency and glutamate. These results suggest that the age-related decrease in neural population spiking, reflected by the decreased offset and decreased glutamate, may contribute to decreased response latency, suggesting adults may need less excitatory neuronal activity in order to perform the task quickly. Similarly, the association between spatial span and decreases in exponent suggest that age related improvement in working memory capacity are supported by the optimization of the balance of excitation and inhibition (Lu et al., 2023; Barak and Tsodyks, 2014; Edin et al., 2009).

While these associations are robust and compelling, we nevertheless recognize that there is a large amount of individual variability in these data, as well as measurement noise that is ubiquitously a problem when relating two different brain measure. A further limitation of this work comes from the superposition and volume conduction of scalp EEG. While we selected six electrodes corresponding to the DLPFC (Herwig et al., 2003) it is important to note that due to known spatial spread and volume conduction of EEG, the spatial specificity of the signal is likely not restricted to DLPFC function but reflects other brain regions as well. While out-of-sample replication is undoubtedly necessary to further support and extend these findings, we are unaware of any other datasets in existence combining both 7 T MRSI and EEG in adolescent populations, and our analysis is therefore limited to the within- sample analysis described in the manuscript.

Together, these findings provide novel *in vivo* evidence describing possible neurobiological mechanisms underlying the maturation of PFC neural function and cognition throughout adolescence. Importantly, these findings are in line with a model of adolescence as a critical period for frontal cortex maturation supporting cognitive development into adulthood (Larsen and Luna, 2018). In this model, developmental changes in glutamate and GABA would drive changes in the E/I balance, supporting maturation of neural activity that supports optimal cognitive control. Developmental disruptions in the development of E/I balance in frontal cortex have been associated with cognitive deficits associated with psychopathology, such as schizophrenia (Hoftman et al., 2017; Vinogradov et al., 2022). Understanding normative PFC development and plasticity can inform mechanisms underlying deviations from normative trajectories and possible interventions.

Resource Sharing Plan

As Dr. Luna and her lab have done throughout our studies, results will be made available to other scientists to further probe our understanding of normative development. Findings will be presented at major meetings relevant to our area of study including: Flux-The International Congress for Integrative Developmental Cognitive Neuroscience, Society for Neuroscience, Organization for Human Brain Mapping, Cognitive Neuroscience Society, and Biological Psychiatry as well as other conferences when the theme includes our area of research (American Psychological Association, Society for Research in Child Development, Society for Research on Adolescence). Results will also be disseminated by Dr. Luna's continuous participation in a variety of related congresses (e.g., Society for Adolescent Health and Medicine); policy related collaborations (e.g., Institute of Medicine – National Academy of Sciences; informing AMA briefs presented to the Supreme Court); and invited lectureships at national and international universities. Dr. Luna is also a responsible contributor to media coverage on human development issues (National Geographic, PBS Brains on Trials, Washington Post, New York Times, as well as smaller pertinent media outlets, such as local newspapers and radio shows). Dr. Luna also presents on a yearly basis to different local high schools and organizations interested in adolescent development. The Laboratory of Neurocognitive Development also has a website where information regarding findings are posted. Finally, Dr. Luna will continue to share her results in Big Data projects where she has

been an organizing member (ADHD200, ABIDE, OpenfMRI, and CoRR) whose aim is to make neuroimaging data available to the scientific community to perform innovative analyses further advancing our understanding. Data and code will be made available upon request.

Funding

This work was supported by MH067924 from the National Institute of Mental Health, T32 Training Grant Number T32MH019986 from the National Institute of Mental Health, F31 Grant Number 1F31MH132246, the Staunton Farm Foundation, and support from the Department of Bioengineering, University of Pittsburgh.

CRediT authorship contribution statement

Chan-Hong Moon: Software, Resources, Data curation. **Hoby Hetherington:** Software, Resources, Data curation. **Will Foran:** Software, Resources, Data curation. **Maria I. Perica:** Writing – original draft, Methodology, Formal analysis. **Shane McKeon:** Writing – review & editing, Writing – original draft, Visualization, Validation, Project administration, Methodology, Investigation, Funding acquisition, Formal analysis. **Finnegan J. Calabro:** Writing – review & editing, Validation, Supervision, Funding acquisition, Conceptualization. **Ashley C. Parr:** Writing – review & editing, Supervision, Conceptualization. **Beatriz Luna:** Writing – review & editing, Supervision, Funding acquisition, Conceptualization.

Declaration of Competing Interest

The authors declare no competing interests.

Data availability

Data will be made available on request.

Acknowledgements

We thank the University of Pittsburgh Clinical and Translational Science Institute (CTSI) for support in recruiting participants, as well as their support by the National Institutes of Health through grant number UL1TR001857. We thank Matthew Missar, Laurie Thompson, Alyssa Famalette, and Vivian Lallo for their work involving our data collection.

Appendix A. Supporting information

Supplementary data associated with this article can be found in the online version at doi:10.1016/j.dcn.2024.101373.

References

Barak, O., Tsodyks, M., 2014. Working models of working memory. Curr. Opin. Neurobiol. 25, 20–24.
Bates, D., Mächler, M., Bolker, B., Walker, S., 2015. Fitting Linear Mixed-Effects Models Using lme4. J. Stat. Softw. 67, 1–48.
Bunge, S.A., Dudukovic, N.M., Thomason, M.E., Vaidya, C.J., Gabrieli, J.D.E., 2002. Immature frontal lobe contributions to cognitive control in children: evidence from fMRI. Neuron 33, 301–311.
Buzsáki, G., Anastassiou, C.A., Koch, C., 2012. The origin of extracellular fields and currents–EEG, ECoG, LFP and spikes. Nat. Rev. Neurosci. 13, 407–420.
Caballero, A., Orozco, A., Tseng, K.Y., 2021. Developmental regulation of excitatory-inhibitory synaptic balance in the prefrontal cortex during adolescence. Semin. Cell Dev. Biol. https://doi.org/10.1016/j.semcdb.2021.02.008.
Calabro, F.J., Murty, V.P., Jalbrzikowski, M., Tervo-Clemmens, B., Luna, B., 2020. Development of Hippocampal-Prefrontal Cortex Interactions through Adolescence. Cereb. Cortex 30, 1548–1558.
Cellier, D., Riddle, J., Petersen, I., Hwang, K., 2021. The development of theta and alpha neural oscillations from ages 3 to 24 years. Dev. Cogn. Neurosci. 50, 100969.
Chattopadhyaya, B., et al., 2004. Experience and activity-dependent maturation of perisomatic GABAergic innervation in primary visual cortex during a postnatal critical period. J. Neurosci. 24, 9598–9611.
Ciesielski, K.T., Lesnik, P.G., Savoy, R.L., Grant, E.P., Ahlfors, S.P., 2006. Developmental neural networks in children performing a Categorical N-Back Task. NeuroImage 33, 980–990.
Colombo, M.A., et al., 2019. The spectral exponent of the resting EEG indexes the presence of consciousness during unresponsiveness induced by propofol, xenon, and ketamine. Neuroimage 189, 631–644.
De Bellis, M.D., et al., 2001. Sex Differences in Brain Maturation during Childhood and Adolescence. Cereb. Cortex 11, 552–557.
De Luca, C.R., et al., 2003. Normative data from the CANTAB. I: development of executive function over the lifespan. J. Clin. Exp. Neuropsychol. 25, 242–254.
Delorme, A., Makeig, S., 2004. EEGLAB: an open source toolbox for analysis of single-trial EEG dynamics including independent component analysis. J. Neurosci. Methods 134, 9–21.
Donoghue, T., et al., 2020a. Parameterizing neural power spectra into periodic and aperiodic components. Nat. Neurosci. 23, 1655–1665.
Donoghue, T., Dominguez, J., Voytek, B., 2020b. Electrophysiological Frequency Band Ratio Measures Conflate Periodic and Aperiodic Neural Activity. ENEURO.0192-20.2020 eNeuro 7. ENEURO.0192-20.2020.
Edin, F., et al., 2009. Mechanism for top-down control of working memory capacity. Proc. Natl. Acad. Sci. 106, 6802–6807.
Fung, S.J., et al., 2010. Expression of Interneuron Markers in the Dorsolateral Prefrontal Cortex of the Developing Human and in Schizophrenia. AJP 167, 1479–1488.
Gao, R., Peterson, E.J., Voytek, B., 2017. Inferring synaptic excitation/inhibition balance from field potentials. Neuroimage 158, 70–78.
Giedd, J.N., 2004. Structural Magnetic Resonance Imaging of the Adolescent Brain. Ann. N. Y. Acad. Sci. 1021, 77–85.
Gogtay, N., et al., 2004. Dynamic mapping of human cortical development during childhood through early adulthood. Proc. Natl. Acad. Sci. U. S. A 101, 8174–8179.
Gold, C., Henze, D.A., Koch, C., Buzsáki, G., 2006. On the origin of the extracellular action potential waveform: A modeling study. J. Neurophysiol. 95, 3113–3128.
Goldman-Rakic, P.S., 1995. Cellular basis of working memory. Neuron 14, 477–485.
Gonzalez-Burgos, I., et al., 2023. Glutamatergic and GABAergic Receptor Modulation Present Unique Electrophysiological Fingerprints in a Concentration-Dependent and Region-Specific Manner. ENEURO.0406-22.2023 eNeuro 10. ENEURO.0406-22.2023.
He, B.J., 2014. Scale-free brain activity: past, present, and future. Trends Cogn. Sci. 18, 480–487.
He, W. *et al.* Co-Increasing Neuronal Noise and Beta Power in the Developing Brain. 839258 Preprint at ⟨https://doi.org/10.1101/839258⟩ (2019).
Hensch, T.K., 2005. Critical period plasticity in local cortical circuits. Nat. Rev. Neurosci. 6, 877–888.
Herwig, U., Satrapi, P., Schönfeldt-Lecuona, C., 2003. Using the International 10-20 EEG System for Positioning of Transcranial Magnetic Stimulation. Brain Topogr. 16, 95–99.
Hetherington, H.P., Avdievich, N.I., Kuznetsov, A.M., Pan, J.W., 2010. RF shimming for spectroscopic localization in the human brain at 7 T. Magn. Reson. Med. 63, 9–19.
Hill, A.T., Clark, G.M., Bigelow, F.J., Lum, J.A.G., Enticott, P.G., 2022. Periodic and aperiodic neural activity displays age-dependent changes across early-to-middle childhood. Dev. Cogn. Neurosci. 54, 101076.
Hoftman, G.D., Datta, D., Lewis, D.A., 2017. Layer 3 excitatory and inhibitory circuitry in the prefrontal cortex: developmental trajectories and alterations in schizophrenia. Biol. Psychiatry 81, 862–873.
Larsen, B. *et al.* A developmental reduction of the excitation:inhibition ratio in association cortex during adolescence. *Science Advances* **8**, eabj8750 (2022).
Larsen, B., Luna, B., 2018. Adolescence as a neurobiological critical period for the development of higher-order cognition. Neurosci. Biobehav Rev. 94, 179–195.
Lindén, H., Pettersen, K.H., Einevoll, G.T., 2010. Intrinsic dendritic filtering gives low-pass power spectra of local field potentials. J. Comput. Neurosci. 29, 423–444.
Lu, L., Gao, Z., Wei, Z., Yi, M., 2023. Working memory depends on the excitatory–inhibitory balance in neuron–astrocyte network. *Chaos: An Interdisciplinary*. J. Nonlinear Sci. 33, 013127.
Luna, B., et al., 2001. Maturation of widely distributed brain function subserves cognitive development. NeuroImage 13, 786–793.
Luna, B., Velanova, K., Geier, C.F., 2008. Development of eye-movement control. Brain Cogn. 68, 293–308.
Luna, B., Marek, S., Larsen, B., Tervo-Clemmens, B., Chahal, R., 2015. An Integrative Model of the Maturation of Cognitive Control. Annu Rev. Neurosci. 38, 151–170.
Mamiya, P.C., Arnett, A.B., Stein, M.A., 2021. Precision Medicine Care in ADHD: The Case for Neural Excitation and Inhibition. Brain Sci. 11, 91.
Manning, J.R., Jacobs, J., Fried, I., Kahana, M.J., 2009. Broadband Shifts in Local Field Potential Power Spectra Are Correlated with Single-Neuron Spiking in Humans. J. Neurosci. 29, 13613–13620.
Mauney, S.A., et al., 2013. Developmental Pattern of Perineuronal Nets in the Human Prefrontal Cortex and Their Deficit in Schizophrenia. Biol. Psychiatry 74, 427–435.
McKeon, S.D., et al., 2023. Age-related differences in transient gamma band activity during working memory maintenance through adolescence. NeuroImage 274, 120112.
McSweeney, M., Morales, S., Valadez, E.A., Buzzell, G.A., Fox, N.A., 2021. Longitudinal age- and sex-related change in background aperiodic activity during early adolescence. Dev. Cogn. Neurosci. 52, 101035.
Merkin, A., et al., 2023. Do age-related differences in aperiodic neural activity explain differences in resting EEG alpha? Neurobiol. Aging 121, 78–87.
Micheva, K.D., Beaulieu, C., 1997. Development and plasticity of the inhibitory neocortical circuitry with an emphasis on the rodent barrel field cortex: a review. Can. J. Physiol. Pharmacol. 75, 470–478.

Miller, K.J., et al., 2012. Human motor cortical activity is selectively phase-entrained on underlying rhythms. PLoS Comput. Biol. 8, e1002655.
Miller, K.J., et al., 2014. Broadband changes in the cortical surface potential track activation of functionally diverse neuronal populations. NeuroImage 85, 711–720.
Miller, K.J., Sorensen, L.B., Ojemann, J.G., Nijs, M., 2009. den. Power-Law Scaling in the Brain Surface Electric Potential. PLOS Comput. Biol. 5, e1000609.
Molina, J.L., et al., 2020. Memantine Effects on Electroencephalographic Measures of Putative Excitatory/Inhibitory Balance in Schizophrenia. Biol. Psychiatry.: Cogn. Neurosci. Neuroimaging 5, 562–568.
Montez, D.F., Calabro, F.J., Luna, B., 2017. The expression of established cognitive brain states stabilizes with working memory development. Elife 6.
Montez, D.F., Calabro, F.J., Luna, B., 2019. Working memory improves developmentally as neural processes stabilize. PLoS ONE 14, e0213010.
Murty, V., Calabro, F., Luna, B., 2016. The Role of Experience in Adolescent Cognitive Development: Integration of Executive, Memory, and Mesolimbic Systems. Neurosci. Biobehav Rev. 70, 46–58.
Onwordi, E.C., et al., 2021. The relationship between synaptic density marker SV2A, glutamate and N-acetyl aspartate levels in healthy volunteers and schizophrenia: a multimodal PET and magnetic resonance spectroscopy brain imaging study. Transl. Psychiatry 11, 1–9.
Ostlund, B.D., Alperin, B.R., Drew, T., Karalunas, S.L., 2021. Behavioral and cognitive correlates of the aperiodic (1/f-like) exponent of the EEG power spectrum in adolescents with and without ADHD. Dev. Cogn. Neurosci. 48, 100931.
Ouyang, G., Hildebrandt, A., Schmitz, F., Herrmann, C.S., 2020. Decomposing alpha and 1/f brain activities reveals their differential associations with cognitive processing speed. NeuroImage 205, 116304.
Pan, J. w, Avdievich, N., Hetherington, H. p, 2010. J-refocused coherence transfer spectroscopic imaging at 7 T in human brain. Magn. Reson. Med. 64, 1237–1246.
Paus, T., Keshavan, M., Giedd, J.N., 2008. Why do many psychiatric disorders emerge during adolescence? Nat. Rev. Neurosci. 9, 947–957.
Peduto, V.A., Concas, A., Santoro, G., Biggio, G., Gessa, G.L., 1991. Biochemical and electrophysiologic evidence that propofol enhances GABAergic transmission in the rat brain. Anesthesiology 75, 1000–1009.
Perica, M.I., et al., 2022. Development of frontal GABA and glutamate supports excitation/inhibition balance from adolescence into adulthood. Prog. Neurobiol. 219, 102370.
Petanjek, Z., et al., 2011. Extraordinary neoteny of synaptic spines in the human prefrontal cortex. PNAS 108, 13281–13286.
Pettersen, K.H., Hagen, E., Einevoll, G.T., 2008. Estimation of population firing rates and current source densities from laminar electrode recordings. J. Comput. Neurosci. 24, 291–313.
Podvalny, E., et al., 2015. A unifying principle underlying the extracellular field potential spectral responses in the human cortex. J. Neurophysiol. 114, 505–519.
Provencher, S.W., 2001. Automatic quantitation of localized in vivo 1H spectra with LCModel. NMR Biomed. 14, 260–264.
Ravindranath, O., Calabro, F.J., Foran, W., Luna, B., 2022. Pubertal development underlies optimization of inhibitory control through specialization of ventrolateral prefrontal cortex. Dev. Cogn. Neurosci. 58, 101162.
Robertson, M.M., et al., 2019. EEG power spectral slope differs by ADHD status and stimulant medication exposure in early childhood. J. Neurophysiol. 122, 2427–2437.
Sahara, S., Yanagawa, Y., O'Leary, D.D.M., Stevens, C.F., 2012. The fraction of cortical GABAergic neurons is constant from near the start of cortical neurogenesis to adulthood. J. Neurosci. 32, 4755–4761.
Salvatore, S.V., et al., 2024. Periodic and aperiodic changes to cortical EEG in response to pharmacological manipulation. J. Neurophysiol. 131, 529–540.
Simmonds, D.J., Hallquist, M.N., Asato, M., Luna, B., 2014. Developmental stages and sex differences of white matter and behavioral development through adolescence: a longitudinal diffusion tensor imaging (DTI) study. NeuroImage 92, 356–368.
Sukenik, N., et al., 2021. Neuronal circuits overcome imbalance in excitation and inhibition by adjusting connection numbers. Proc. Natl. Acad. Sci. USA 118, e2018459118.
Tada, M., et al., 2020. Gamma-Band Auditory Steady-State Response as a Neurophysiological Marker for Excitation and Inhibition Balance: A Review for Understanding Schizophrenia and Other Neuropsychiatric Disorders. Clin. EEG Neurosci. 51, 234–243.
Tervo-Clemmens, B. *et al.* A Canonical Trajectory of Executive Function Maturation During the Transition from Adolescence to Adulthood. PsyArXiv (2022) doi: 10.31234/osf.io/73yfv.
Tingley, D., Yamamoto, T., Hirose, K., Keele, L. & Imai, K. Mediation: R package for causal mediation analysis. (2014).
Tröndle, M., Popov, T., Dziemian, S., Langer, N., 2022. Decomposing the role of alpha oscillations during brain maturation. eLife 11, e77571.
Uhlhaas, P.J., Roux, F., Rodriguez, E., Rotarska-Jagiela, A., Singer, W., 2010. Neural synchrony and the development of cortical networks. Trends Cogn. Sci. 14, 72–80.
Vinogradov, S., Chafee, M.V., Lee, E., Morishita, H., 2022. Psychosis spectrum illnesses as disorders of prefrontal critical period plasticity. Neuropsychopharmacol 1–18. https://doi.org/10.1038/s41386-022-01451-w.
Voytek, B., et al., 2015. Age-Related Changes in 1/f Neural Electrophysiological Noise. J. Neurosci. 35, 13257–13265.
Waschke, L., et al., 2021. Modality-specific tracking of attention and sensory statistics in the human electrophysiological spectral exponent. Elife 10, e70068.
Whitford, T.J., et al., 2007. Brain maturation in adolescence: Concurrent changes in neuroanatomy and neurophysiology. Hum. Brain Mapp. 28, 228–237.
Wilkinson, C.L., Nelson, C.A., 2021. Increased aperiodic gamma power in young boys with Fragile X Syndrome is associated with better language ability. *Molecular.* Autism 12, 17.
Wood, S.N., 2013. A simple test for random effects in regression models. Biometrika 100, 1005–1010.
Wood, S.N., 2017. Generalized Additive Models: An Introduction with R. Chapman and Hall/CRC, New York. https://doi.org/10.1201/9781315370279.
Zhang, Z., Jiao, Y.-Y., Sun, Q.-Q., 2011. Developmental maturation of excitation and inhibition balance in principal neurons across four layers of somatosensory cortex. Neuroscience 174, 10–25.